Tuning the bandgap and absorption behaviour of the newly-fabricated Ultrahigh Molecular weight Polyethylene Oxide- Polyvinyl Alcohol/ Graphene Oxide hybrid nanocomposites

Nisreen R Aldulaimi[1,2] and Ehssan Al-Bermany[1] (ORCID)

Abstract

Graphene nanosheets are promising nanofillers to the tunable structure, properties of materials, and optical bandgap. This search focuses on investigating the new nanocomposites of Ultra-high molecular weight polyethylene oxide (UHMWPEO) with different loading ratios of polyvinyl alcohol (PVA) reinforced with graphene oxide (GO) by applying the modified solution-sonication-casting method. Fourier-transform infrared spectroscopy (FTIR) shows strong interfacial interaction between the blended polymers and GO nanosheets in the nanocomposites. X-Ray diffraction (XRD) reveals a significant shifting in the PEO and reduction in the crystallinity. Optical microscopy (OM) images exhibit fine homogeneity of the polymer in the matrix with excellent dispersal of GO in nanocomposites as supported by scanning electron microscopy (SEM). Attractively, the samples with a higher ratio of UHMWPEO exhibit better optical behavior, and great improvements were presented after the contribution of GO. UV-visible spectroscopy has characterized the absorption, absorption co-efficient, real and imaginary, bandgap, and other parameters. The allowed bandgap was significantly enhanced by reducing up to 80%, whereas the forbidden bandgap was improved by up to 160% of the nanocomposites. Additionally, nanocomposites exhibited significant adsorption of radiation-ray, especially after the contribution of GO. The findings are promising as various applications could come to the fore: radiation protection, spectroscopy devices, and other applications.

Keywords

UHMWPEO, polyvinyl alcohol, graphene oxide, optical properties, nanocomposites, bandgap, radiation

Received 30 June 2021; accepted 15 June 2022

Introduction

Nanocomposites are an important subject in developing and producing materials, particularly polymer-nanomaterials.[1] It is well recognized that the most significant factors resulting from the interaction of filler nanoparticles with polymer are nanocomposites that improve nanocomposites' properties in nuclei.[2] Polymer nanocomposites attract great interest because these materials possess a high potential for a big improvement in properties by adding a slight number of nanoparticles to the polymer arrays.[3,4] Nanocomposite materials are a novel class of materials that have more properties than their constituents. The addition of a small number of nanoparticles may vastly boost several properties while sacrificing none of the polymer's lightweight matrices[3] and overcoming several polymer weaknesses. The few atomic layers of the 2D materials attract substantial and outstanding attention to their multipurpose chemical and physical properties.[5,6] For instance, graphene and its derivative are the 2D material that was first experimentally prepared and dominated research in the recent decade.[7–10] As

[1]Department of Physics, College of Education for Pure Science, University of Babylon, Babylon, Iraq
[2]Educational Directorate of Babylon, Ministry of Education, Babylon, Hillah, Iraq

Corresponding author:
Ehssan Al-Bermany, Department of Physics, College of Education for Pure Science, University of Babylon, Babylon-Najaf Main Rood, Babylon, 50001, Iraq.
Email: ehssan@itnet.uobabylon.edu.iq

graphene oxide nanosheets have unique characteristics that could bring notable improvement to nanocomposites.[11] Mostly, it is easily functional in wide and various spintronics, electronics, and photoelectronic, applications, etc.[12,13]

Polyethylene oxide (UHMWPEO) is the most widely used material in artificial joints among hard-on-soft bearings.[14] It is an engineering polymer that differs in terms of average chain length and average molecular weight.[15] UHMWPEO is water-soluble and commonly used in several different applications as functional additives, such as flocculation methods, wastewater treatment, mining, food processing, cosmetics, and coagulation.[16] Poly (vinyl alcohol) (PVA) by a suspended hydroxyl collection has a relatively simple chemical structure. There are commercial PVA modifiers with high grades of hydrolysis.[17] The grades of hydrolysis, or the number of acetate collections in the polymer,[18] have an impact on its biochemical properties, solubility, and PVA crystallization.[19] It is eminent from other polymers of good properties such as wear resistance, strength, thermal stability, and quality.[20]

Several studies[21–23] had listed some very interesting findings when PEO and PVA polymers were formed with each other as a polymer mixed with graphene oxide or with other nanoparticles. Whereas the Ultra-high molecular weight PEO (UHMWPEO) that was used in this study does not address it before, to the best of our knowledge, or with PVA or GO nanosheets. Yuan-Cheng Cao et al., (2011)[23] used a PEO and GO nanocomposite film targeted without chemical changes, and low-temperature polymer fuel cells. SEM morphology images show the composite material without defects in the structure of the PEO/GO membrane. Small-angle XRD outcomes for the film samples indicate a reflection of the d-spacing (001) of GO in the PEO matrix. This peak is changed from 11° to 4.5^{o} of the PEO samples after the addition of the GO layers. The PEO/GO membrane's ionic conductivity rises from 0.086 to 0.134 S cm^{-1} when the activity with relative humidity and the temperature rises from 25 to 60 ^{o}C of 100%. Additionally, the measurements illustrate the electronic resistance to DC at room temperature and 100% relative humidity of this film that is greater than 20 M. Shujahadeen B. Aziz1 and co-others (2017),[22] investigated the optical properties of PEO and PVA-PEO blended polymer using two procedures to determine the optical band gap and evaluate the types of electronic transitions. The well-established solution cast technique was prepared with a solid electrolyte blended polymer that is movies based on PVA: PEO. The absorption increased and shifted to higher wavelengths as the aluminum salt concentration increased. Lowering the energy band gap by shifting the absorption edge to lower photon energy shows high reactivity between the aluminum salt with the blended polymers. The doped samples display an increase in refractive index. Many studies extendedly investigate the mixing of this polymer with several nanomaterials and investigate their applications.

Despite all the previous studies, this PEO with ultra-high molecular weight (5 000 000 g mol^{-1}) is not characterized, investigated, or mixed with other polymers or nanomaterials to the best of our knowledge. This investigation is the first study that could give a good opportunity to unravel this material and display the molecular weight influence in comparison with other studies. Therefore, this investigation focuses on fabricated new nanocomposites using UHMW-PEO: PVA that was mixed firstly with different ratios from both polymers, then reinforced with graphene nanosheets using the advanced acoustic mixing method. The fine dispersion of GO and the fine homogeneous mixture of polymers were obtained in the matrix. PVA with a different loading proportion was used to ameliorate UHMWPEO properties and increase the cross-linkage amongst UHMWPEO and graphene nanoscale panels. FTIR, OM, and UV-Visible Spectrophotometer were used to characterize the effect of GO nanosheets on the tunable bandgap and optical behavior of the new nanocomposites.

Experimental part

Materials

Sigma-Aldrich company in the UK was supplied with the high molecular weight PEO (5 000 000 g mol^{-1}) and graphite powder (40 M), as well as other materials for graphene preparations. Media Labs Pvt. Dindori, Nashik, India provided PVA with a molecular weight (160,000) gm^{-1}.

Methods

Graphene oxide purification. GO was synthesized according to modified Hummer[24] methods, which are explained briefly in the support information Figure (1S), in addition to the characterizations of synthesized GO. The procedure of syntheses of GO followed the method described in our previous publication.[25]

Purification of the nanocomposites. UHMWPEO and PVA were thrown in distilled water separately using a magnetic stirrer under 50 ^{o}C firstly, and then it was mixed applying several different proportions as UHMW-PEO: PVA (87.5:12.5, 75:25, and 62.5:37.5 wt. %), these mixing ratio samples were fully homogenous, whereas using ratio of PVA equal and above than 50 wt. % show separation after leaving the samples for a few hours. GO was added with 1 wt. % for the samples to fabricate the new nanocomposites.

All sample was mixed for 20 h without heat, and then GO was added after sonication for 15 min. The samples followed developed processes such as dissolved sonicating and mixing. Where firstly, polymers were dissolved separately and then mixed until getting fully dissolved in each other. The sample was left for 24 h to be sure the blended polymers were cross-linked and fully homogeneous, whereas other separated samples had a PVA ratio equal to above 50 wt. % were suspended from this study because it was not homogeneous with separation in some parts. GO was added to the fully dissolved polymer

Table 1. The purification method of samples.

Sample	Con. Wt. %			Mixing time, h	Sonication time, h	Dry method
	PVA	PEO	GO			
GO	0	0	100	4	4	Freeze drier
P1	12.5	87.5	0	20	0	Under air for 168 H
P2	25	75	0	20	0	
P3	37.5	62.5	0	20	0	
NC1	12	87	1	27	2	
NC2	24.5	74.5	1	32	2	
NC3	36	63	1	32	2	

and then mixed with sonication several times for 15 min, followed by mixing using a magnetic stirrer for 2 h. This operation was carried out several times to get better dispersion and homogeneousness of the nanomaterials in the matrix as summarized in Table 1. Finally, homogeneous mixtures were cast into a plastic Petri dish and allowed to dry under air.

Characterizations. Fourier Transforms Infrared (FTIR) made by Bruker Company, Germany, model (vertex 70) is working in the range between 4000 -500 cm^{-1}. XRD Diffraction manufactured by Phillips Company in Holland, model Xpert was used to characterize the samples. UV-Visible double beam spectrophotometer model (Vertex 701) is used to characterize the optical properties in the region between (4000–400) cm^{-1} that is manufactured by Phillips company, Japan. The optical microscope (OM) model (Nikon - 73,346) made in Japan by Olympus Company was used to capture the optical images of the samples with a magnification of 40X. Filed Effect Scanning Electron Microscopy (FESEM) made by Tescan company, France, model Mira-3, and within (1.2 nm at 30 kV) and (2.3 nm at 3 kV). In addition, the source of Sr-90 with 0.1 μ CI, 28.6 years radioactivity activity of Beta radiation was pleased 7 cm away from the counter, which is the Geiger detector. The samples were delighted 3 cm away from the source to measure the absorption of the samples to the Beta radiation.

Theoretical calculations

The ratio between the intensity of absorbed light (I_A) on the incident light (I_o) of a material is known as absorbance (A).[26]

$$A = \frac{I_A}{I_0} \tag{1}$$

The transmittance spectra (T) are calculated from the below relationship.[26]

$$T = e^{-\alpha t} \tag{2}$$

The absorption factor (α) (cm)$^{-1}$ is considered from the Lambert bear formulation[27]

$$\alpha = 2.303 \cdot A/t \tag{3}$$

The optical energy gap allowed and prohibited indirect UHMWPEO-PVA and UHMWPEO -PVA/GO nanocomposites were measured from both the interception of the extrapolated linear component as well as the photon energy using formula[4] ($h\upsilon$) at $(ah\upsilon)^{1/n} = 0$.[28]

$$ah\upsilon = B(h\upsilon - E_g)^{\mathrm{r}} \tag{4}$$

Where *(B)*, *(h)*, *(υ)*, *(E_g)*, and (r) are constant, Planck's constant, frequency, the energy of phonon, and the exponential constant. (r) could represent a variety of values, for instance, 1/2 and 3/2, or could be two and three for allowed and forbidden direct or indirect transitions, respectively, depending on the transition formulation.[29]

(n) is the index of refractive and (k) the coefficient of extinction of the film that was considered from the following calculations.[29]

$$n = \frac{1+R}{1-R} + \left[\frac{4R}{(1-R)} - K^2 \right]^{1/2} \tag{5}$$

$$K = \frac{\alpha\lambda}{4\pi} \tag{6}$$

Where (R) means the reflectance and (λ = 1.5406) A°, which means the wavelength straight of the Cu Kα.[26] The complex dielectric constant can be described as in the equation.

$$\varepsilon = \varepsilon_r + \varepsilon_i \tag{7}$$

$$\varepsilon_r = n^2 - k^2 \tag{8}$$

$$\varepsilon_i = 2nk \tag{9}$$

Where ε_r denotes the real part of the dielectric constant and ε_i denotes the imaginary part.[29]

Results and discussions

Figure 1 shows the FTIR spectra of UHMWPEO-PVA blended polymers and UHMWPEO-PVA/GO nanocomposites with various mixing ratios of polymers. It was recorded between the ranges of (4000–500) cm^{-1} wavenumber. FTIR spectra of the (PEO-PVA) appeared at 2882 cm^{-1} of (methyl C-H symmetric stretch), 1340 cm^{-1} of (C-H$_3$ links), 3285 cm^{-1} of (O-H) bond, 1716 cm^{-1} of (C=O) bond, 1278 cm^{-1} of (O-H) bond, 959 cm^{-1} of (C-H) bond, and 1092, and 840 cm^{-1} of (C-O) bond. These peaks show a good and strong interaction between polymers and confirm the preparation of strongly bonded polymers in comparison with the polymer results, and these results are in agreement with the other finding.[23,25]

The contribution of the GO nanosheets sheets exhibited notable strong interfacial integration that was associated with shifting the most peaks from their positions, in addition, to change in the intensity to higher intensity, such as (C-H$_2$) methylene, C-H symmetric stretch, and carbonyl (C=O) at the peaks (2880, 1716, and 1466) cm^{-1}, in addition to (C-H$_3$, O-H, and C-O-C,) bands links for peak position (1341, 1278 and 1095) cm^{-1} respectively, as presented in Figure 1. This interaction could be associated with the formulation of the intermolecular hydrogen bonding among these polymers and the functional site on the surface of GO nanosheets in strong agreement with other researchers finding.[30,31] Moreover, this interaction is reported between the ether collection (C–O–C) sites of PEO with the carbonyl groups C=O and –OH as the polar functional groups of GO nanosheets.[25,32]

The XRD analysis is employed to examine the material structure and determine whether they are crystalline or amorphous. Figure 2 displays the X-ray spectra of UHMWPEO and PVA pure and after blending with GO. The GO showed a sharp peak at $2\theta = 11°$ associated with the (002) deflection of the GO chips, in agreement with the literature.[33] The GO peaks that are not
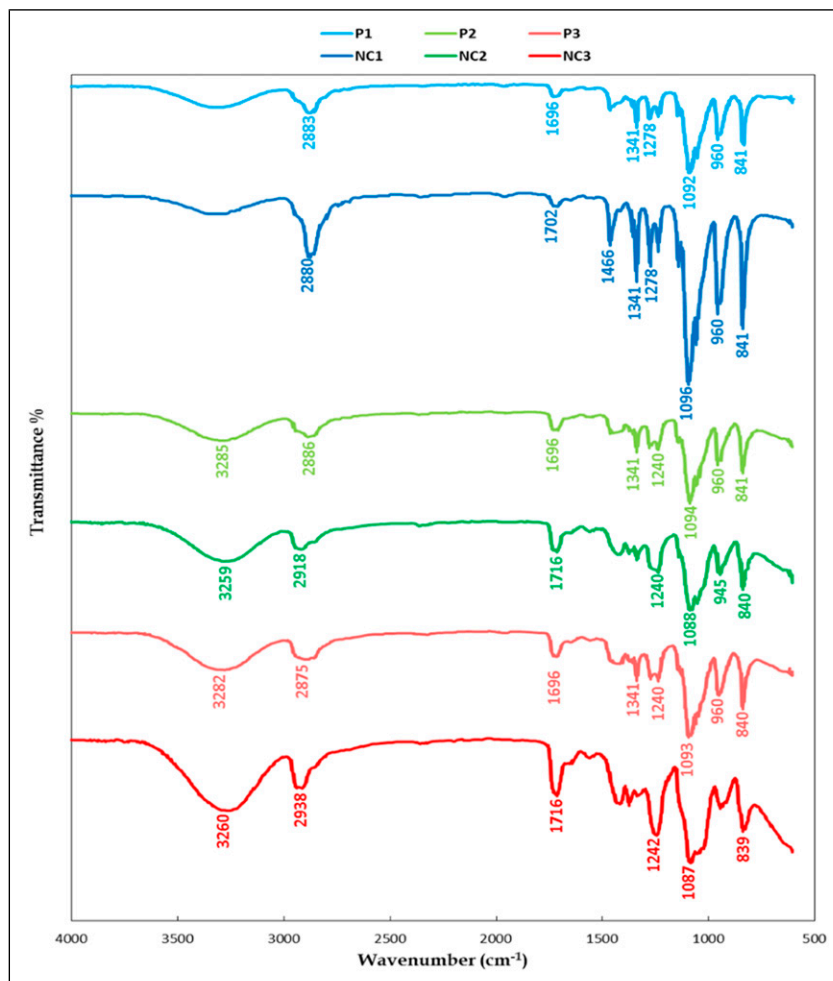

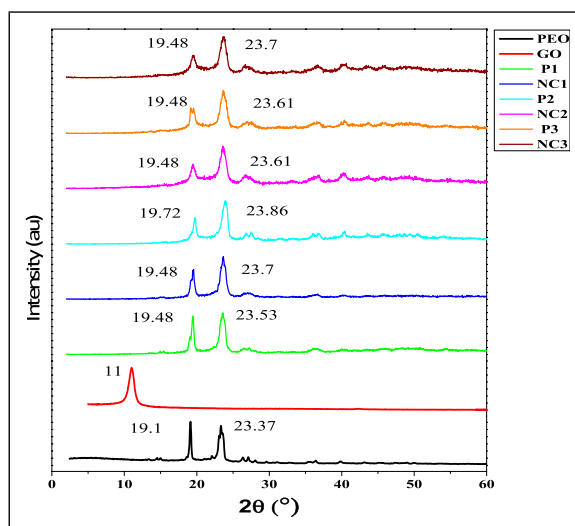**Figure 1.** FTIR spectra of (UHMWPEO-PVA) blended polymers and (UHMWPEO-PVA/GO) nanocomposites.

Figure 2. XRD patterns of PEO, GO, blended polymer, and nanocomposites.

presented in the samples could be related to the low loading ratio or orientation of nanosheets in agreement with the other finding.[34] The PEO pattern showed peaks at 19.1° and 23.37°, which correlated with (120) and (112). This could be the main reason to overlap and disappearance due to the high intensity of PEO peaks and strong interaction. This is presented through the significant shift of the PEO peak to 19.48° and 23.53° after the loading ratio of PVA with 12.5 wt. %. Additionally, the contribution of graphene oxide with 1 wt. % revealed another shifting in the second to 23.7°, compared with the pure PEO.

The increase of the PVA ratio to 25 wt. % in the matrix exhibited another notable shifting in peaks position to 19.7° and 23.86°. Whereas the contribution of GO was shifted to 19.48° and 23.61°. The addition of PVA and the contribution of GO revealed a reduction in the peak intensity compared with the PEO peaks, where this behviour is reported by other investigations.[25,35]

Interestingly, this shifting was continuous with increasing the PVA to 37.5 wt. %, where the PEO peaks were shifted to 19.48° and 23.61°, whereas the contribution of GO revealed another shifting and 23.7. The addition of PVA and the contribution of GO revealed a reduction in the intensity of the peaks compared with the net of PEO peaks. Therefore, the crystallite size (D) in (nm) of the sample peaks was estimated from the Scherer formula (10).[5]

$$D = \frac{K\lambda}{\beta cos(\theta)} \tag{10}$$

Where (K) means the shape factor of the average crystallite (~0.9), (β) means the full width at half-maximum of crystalline material peak (FWHM), (λ) means the incident wavelength of X-ray (nm), and (θ) means the Bragg angle, where Bragg formal used to calculate the d-spacing (nm).

With the contribution of the GO at the nanoscale levels, the effect of the average crystal size of blended polymer PEO-PVA showed a slight decrease compared to the PEO; moreover, the contribution of GO showed another reduction in the crystallinity size of the nanocomposites compared to the blended polymer PEO-PVA and the net of PEO as shown in Table 2, these findings are strongly agreed with the literature.[2,3]

Figure 3 reveals the optical microscopy images (OM) of UHMWPEO-PVA films and UHMWPEO-PVA/GO nanocomposites with different UHMWPEO and PVA mixing ratios with 40X magnification. The images clearly show the fine homogeneous matrix of the blended polymers, with a good dispersal of GO in the nanocomposites films. OM photo showed that this method was fully successfully fabricated the blended polymers and nanocomposites. Moreover, the NC1, which included the higher ratio of UHMWPEO illustrated the best distribution of GO in the matrix. GO contribution resulted in significant changes in these films without aggregation or affecting the optical transparency of the prepared nanocomposites in agreement with the works of literature.[26,36]

The UV-Visible absorption spectra of PEO-PVA blended polymer and nanocomposites were characterized in the region (200–1100) nm wavelength that is exhibited in Figure 4(a). At 200 nm, the blended polymer samples exhibited absorption peaks. Interestingly, samples that contained a higher ratio of PEO exhibited better adsorption behavior, where P1 revealed the best results compared with other blended polymers. Meanwhile, the contribution of GO showed notable enhancement in the absorption behavior of all the nanocomposites. For comparison, the absorption of samples was calculated at 600 nm to find the improvement of absorption that exhibited enhanced up to 37%, 33%, and 44% of the NC1 and NC2, and NC3 compared with the P1, P2, and P3, respectively. However, NC1 presented the best absorption behavior in comparison with nanocomposites and blended polymers.

Remarkably, the nanocomposites displayed a small peak shoulder at 270 nm that was not revealed in blended polymers. Generally, the covalent bonding interactions or π–π stacking is in the main conjected of GO with the blended polymers that are causing a strong absorption band of 200–300 nm. Where, at 200 nm, the peak transition of plasmonic π-π* (C=C) is the

Table 2. Summarized the (K), (β), (λ), and (θ) of the PEO, blended polymer, and nanocomposites.

Samples	Peaks	1	2
PEO	θ (°)	11.85	9.55
	β (°)	0.82	0.286
	d-spacing (nm)	3.756	4.652
	D (nm)	1.728	4.914s
P1	θ (°)	11.765	9.74
	β (°)	0.881	0.39
	d-spacing (nm)	3.783	4.556
	D (nm)	1.607	3.609
NC1	θ (°)	11.85	9.74
	β (°)	0.883	0.609
	d-spacing (nm)	3.756	4.556
	D (nm)	1.604	2.279
P2	θ (°)	11.94	9.86
	β (°)	0.97	0.543
	d-spacing (nm)	3.728	4.502
	D (nm)	1.46	2.595
NC2	θ (°)	11.767	9.74
	β (°)	1.15	0.979
	d-spacing (nm)	3.783	4.556
	D (nm)	1.229	1.437
P3	θ (°)	11.85	9.74
	β (°)	1.088	0.883
	d-spacing (nm)	3.756	4.556
	D (nm)	1.302	1.593
NC3	θ (°)	11.96	9.74
	β (°)	1.15	0.926
	d-spacing (nm)	3.719	4.556
	D (nm)	1.23	1.519
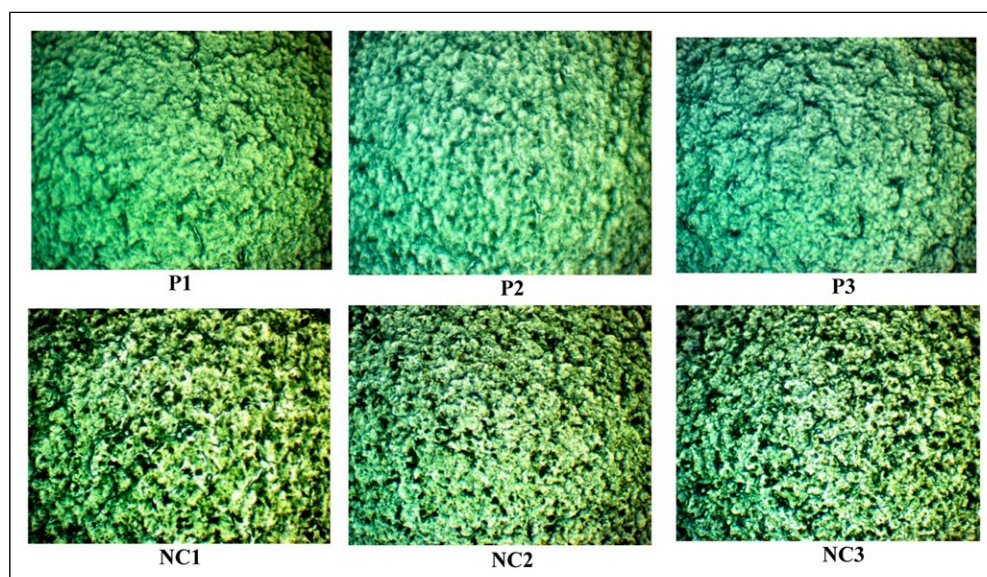
Figure 3. Optical microscopy (OM) images of (UHMWPEO-PVA) films and (UHMWPEO-PVA/GO) nanocomposites with (40X) magnification.

responsibility of the absorption peak of the prepared GO meanwhile the presented shoulder at around 270 nm is conjunctive to the n-π* (C=O) transition.[37] The slowly re-shifted of the plasmonic peak exhibited from 200 nm to 270 nm; this shifting could be increased by increasing the reaction time.[38] The rise in the percentage of the carbon atoms sp^2 hybridized could attribute to this shifting, and this behavior is agreed with the literature.[37] Therefore, in the visible light band, the GO absorption is presented as much greater than the absorption of blended polymers.

Figure 4(b) displayed the absorption coefficient with the incident photon energy of the UHMWPEO-PVA films and UHMWPEO-PVA-GO nanocomposite. Interestingly, the blended polymers P1 that consist of a higher ratio of UHMWPEO presented better absorption behavior in comparison with other blended polymers. Meanwhile, the incorporation of graphene oxide nanosheets is associated with a notable increase in absorption coefficient in comparison with the blended polymers. Moreover, NC1, which contains the higher ratio of UHMWPEO, also exhibited the best adsorption behavior in contrast with all other samples. This behavior indicates a high potential for electron transfer, and that increased with increasing the UHMWPEO ratio and GO contribution with increasing the energy. This shows these factors are very important to consider during the fabrication of nanocomposites.

This finding could use the NC1 to infer the nature of direct electron transport for electron transport is the conductivity of (UHMWPEO-PVA/GO) nanocomposites at the expected energy frequency when the absorption coefficient value is low, and electrons and photons can conserve energy and momentum. The results indicate that the absorption coefficient of the (UHMWPEO-PVA/GO) nanocomposites had values smaller than 104 cm^{-1} which means it is an indirect gap, in accord with the literature.[39] When the level of energy is low, the absorption tends to decrease, which indicates the electron transitions were low. Generally, this performance was changed with increasing the energy of a photon, this indicates a high potential for electron transfer.[40,41]

Figure 5(a) and (b) show the differences between $(\alpha h\upsilon)^{1/2}$ and $(\alpha h\upsilon)^{1/3}$ absorption edges of the UHMWPEO-PVA blend polymer and UHMWPEO-PVA/GO nanocomposites as a photon energy function. Drawing a straight line starting from the top of the curve to the direction of the (X) axis at the value $(h\upsilon)^r = 0$ yields the indirect (tolerable) energy gap transition.[5] $(h\upsilon)^{1/2} = 0$, $(h\upsilon)^{1/2} = 0$, and $(h\upsilon)^{1/2} = 0$, it can show that the energy gap and permissible values of the UHMWPEO-PVA mixture decreased in the samples.

The blended polymer contained a higher PEO ratio and showed enhancement in the energy gap result, where P1 was the better result in comparison with other blended samples than P2 and P3, whereas P2 exhibited a better result than P3. Meanwhile, this behavior was significantly enhanced after the addition of GO nanosheets, where all the nanocomposites were turned to exhibit values less than 3 eV of the energy gap compared with blended polymers. NC1 exhibited the best reduction and value in comparison with other samples, as shown in Table 3. Where GO exposed outstanding tunable of the energy gap where it turns the blended polymer form insolated to semiconductor materials of all the nanocomposites. Where the allowed bandgap was significantly enhanced by reducing up to 79%, 58%, and 80%, whereas the forbidden bandgap improved up to
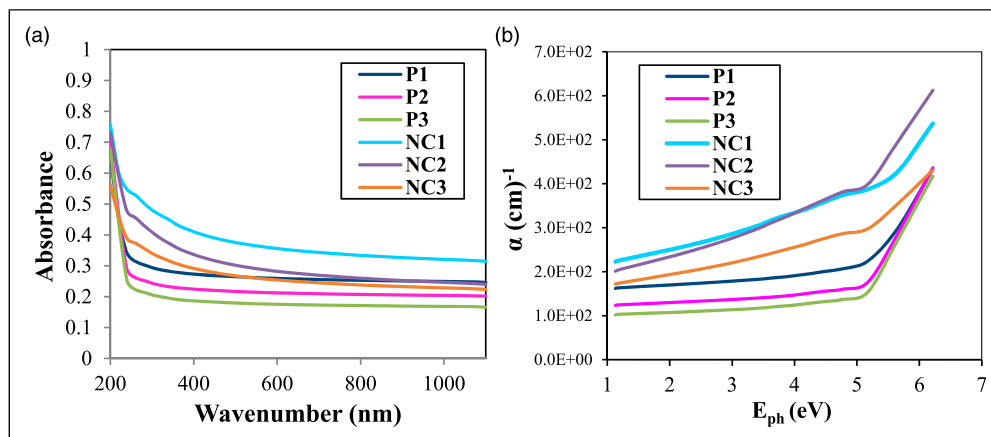

Figure 4. (a) The absorbance spectra with the wavelength and (b) The absorption coefficient with the photon energy of UHMWPEO-PVA and UHMWPEO-PVA/GO nanocomposite.
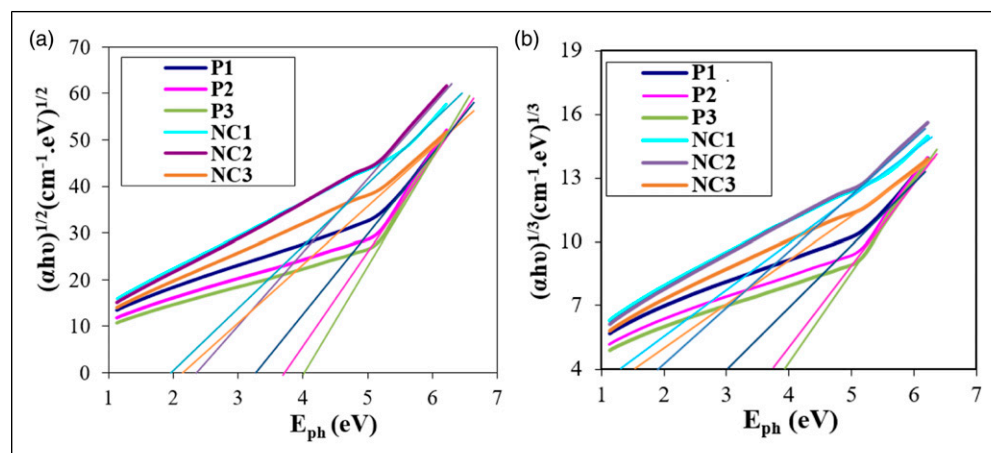

Figure 5. (a) The optical energy gap for the allowed direct transition $(\alpha h\upsilon)^{1/2}$ and (b) the forbidden direct transition with the photon energy of UHMWPEO-PVA films and UHMWPEO-PVA-GO nanocomposites.

130%, 90%, and 160% of the NC1, NC2, and NC3 compared with their blended polymers P1, P2, and P3. The adjustable bandgap showed a significant decrease in the energy gap values in accord with the literature.[41] They reported that the change in the bandgap results associated with an alteration of the GO bandgap through introducing modifications in the structure with the additional functional groups of GO. Where the addition of new oxygen assumes to split the graphitic carbon regions into smaller segments as graphitic islands that true to increase the bandgap, this result is supported by semi-empirical modeling done of the GO flakes with different graphitic island sizes; this defines the scenario providing band gap values, thus following the experimental emission energies trend.[5,41,42]

Figure 6 demonstrates the changes in the extinction coefficient of the (UHMWPEO-PVA) nanocomposites with wavelength. With the addendum of graphene oxide nanoparticles to the polymer mixture, the extinction coefficient results of blended polymers enhanced with the rise of the PEO ratio in the samples. Further, graphene oxide nanosheets can alter the composition of the polymer mixture (PVA - PEO). In addition, GO significantly increased the absorption, and accordingly, the extinction coefficient increased. This is because the absorption coefficient and the extinction coefficient have a close relationship number.[6] The best results were obtained for the compound P1, and NC1 in comparison with other polymers, and this behavior is agreed with the literature.[5,43]

The changes in the real and imaginary dielectric constant with the wavelength of UHMWPEO-PVA films and UHMWPEO-PVA/GO nanocomposites are illustrated in Figure 7(a) and (b). These figures exhibited the real and fictional

Table 3. The optical energy gap of samples.

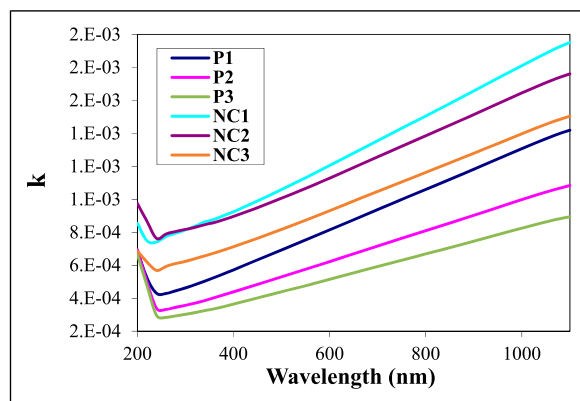| Sample code	Direct transition (Ev)	
	Allowed	Forbidden
P1	3.4	3
P2	3.8	3.6
P3	4	3.9
NC1	1.9	1.3
NC2	2.4	1.9
NC3	2.2	1.5

Figure 6. The Extinction Factor (K) of UHMWPEO-PVA films and UHMWPEO-PVA/GO nanocomposites with the wavelength.
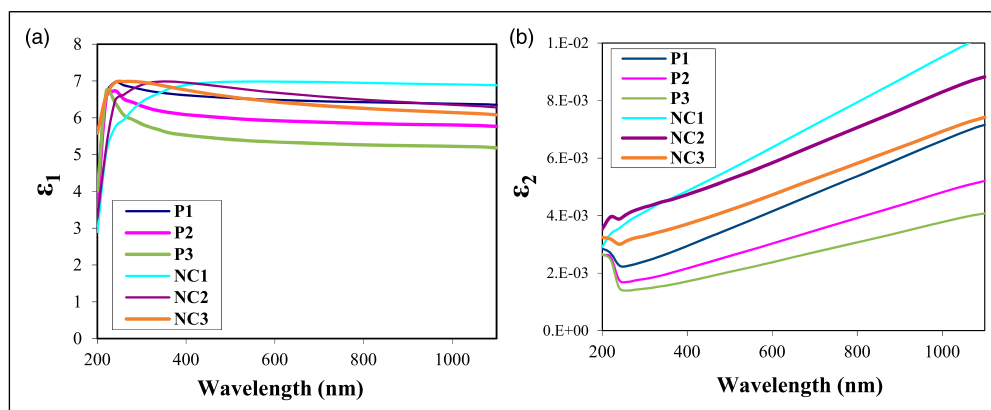

Figure 7. (a) The real dielectric constant and (b) the imaginary dielectric constant of UHMWPEO-PVA films and UHMWPEO-PVA/GO nanocomposites with the wavelength.

parts of the dielectric constants of the UHMWPEO-PVA mixture were improved. The best results exhibited that the P1 revealed the better results. Meanwhile, the addition of GO nanosheets should significantly improve all results and the best results were obtained for the NC1 nanocomposites. That is due to the increase in the electrical polarization of the nanocomposites after the addition of graphene oxide nanostructures and a higher concentration of PEO, this also improved the isolation constants, both real and theoretical. This behviour of constants comes in agreement with the literature[26] after loading the GO in the different molecular weights of PEGs.

Figure 8 displays the transmittance (T) spectra of the PVA- UHMWPEO and PVA- UHMWPEO/GO nanocomposites as a function of wavelength, showing that the permeability of all samples increased rapidly as the wavelength was increased to about 240 nm, then remained nearly constant after 260 nm. The best absorption results were exhibited in the PVA-PEO mixture (P1) and their nanocomposites (NC1). The results clearly showed that GO affects the reduction of light transmittance but does not affect the transparency of the composites,[26,36] this behavior is consistent with the literature.[44]

The surface morphology of blended polymers and nanocomposites was examined using a FESEM as shown in Figure 9. FESEM images of the surface morphology of the blended polymer revealed a grainy and rough that were accumulations of homogeneous films. The contribution of GO nanosheets in the polymer matrix of the nanocomposites displayed good dispersion and granular structure with some aggregations of particles due to the van der Waals forces, whereas most of the GO nanosheets were well-scattered and densely dispersed on the surface of the nanocomposite films with well-distributed of GO nanosheets into the surface that indicated changes in surface shape. This may imply a homogeneous growth mechanism. The results confirm the researchers' findings and optical microscopy images. The FESEM pictures (G and H) in Figure[12] depicted the GO size measurements ranging from a few nanometers to a few microns.

Figure 10 revealed the ability of newly fabricated nanocomposites to adsorb the radiation. Figure 10(a) and (b) illustrates the Ln of radiation attenuation (N) with the increasing the PVA ratio of PEO-PVA blended polymer and nanocomposites. It is noticed the new fabricated blended polymer was adsorbed to the radiation ray. Moreover, the contribution of GO nanosheets has significantly enhanced the adsorption of the ray radiation compared with the blended polymers. Radiation attenuation was calculated using formula (11).[45]

$$N = N_o exp^{(-\mu x)} \tag{11}$$

(N_o) indicates the number of particles of radiation passing without any sample, (N) is the number of radiation particles passing through the thickness (x) of the absorber to be counted during a specified period, and (μ) the irradiation attenuation coefficient of the source.[45] The shape of lateral scattering reduces the absorption according to Lambert's law.[5] In Figure 10(c), the attenuation of the radiation coefficient showed a significant rise in the GO involvement in the nanocomposites compared with the blended polymers. Since ray shielding requires materials with many mass, density, and atomic numbers, the inclusion of GO nanosheets in each region improves protection. A radiation ray pathway is included. The ability to absorb radiation rays as they pass through nanocomposites results in an exponential reduction even with a low loading ratio of GO these results are matched literature.[5] Interestingly, the sample with a higher ratio of UHMW-PEO (P1 and NC1) exhibited the best adsorption of radiation ray in both blended polymer as well as the nanocomposites, whereas increasing the PVA loading ratio displayed redaction in the results in agreement and support the finding of the optical properties behavior. These nanocomposites are promising for light radiation protection such as making a shield, suits, and glasses for workers in X-Ray and radiation laboratories containing radiation, additionally, it is could be promising for landfilling radioactive waste or the chemical nuclear through mixing it is with light concrete that uses in to enhance the effectiveness of samples to absorb the radiation, X-ray, and UV ray, etc.

As exposed in Figure 10(c), the mass attenuation coefficient depends on the compositions of the shielding material and the incident photon energy. Where the mass attenuation coefficient increases considerably after the contribution of GO in the nanocomposites in comparison with the polymer matrix. This can be explained through the three main photon interactions
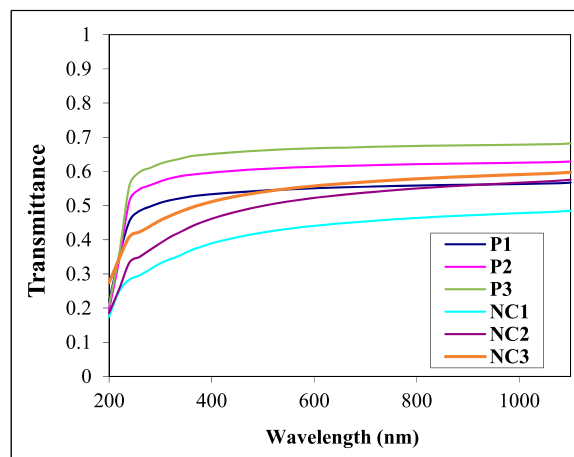

Figure 8. The transmittance spectrum of UHMWPEO-PVA films and UHMWPEO-PVA/GO nanocomposites with a wavelength.
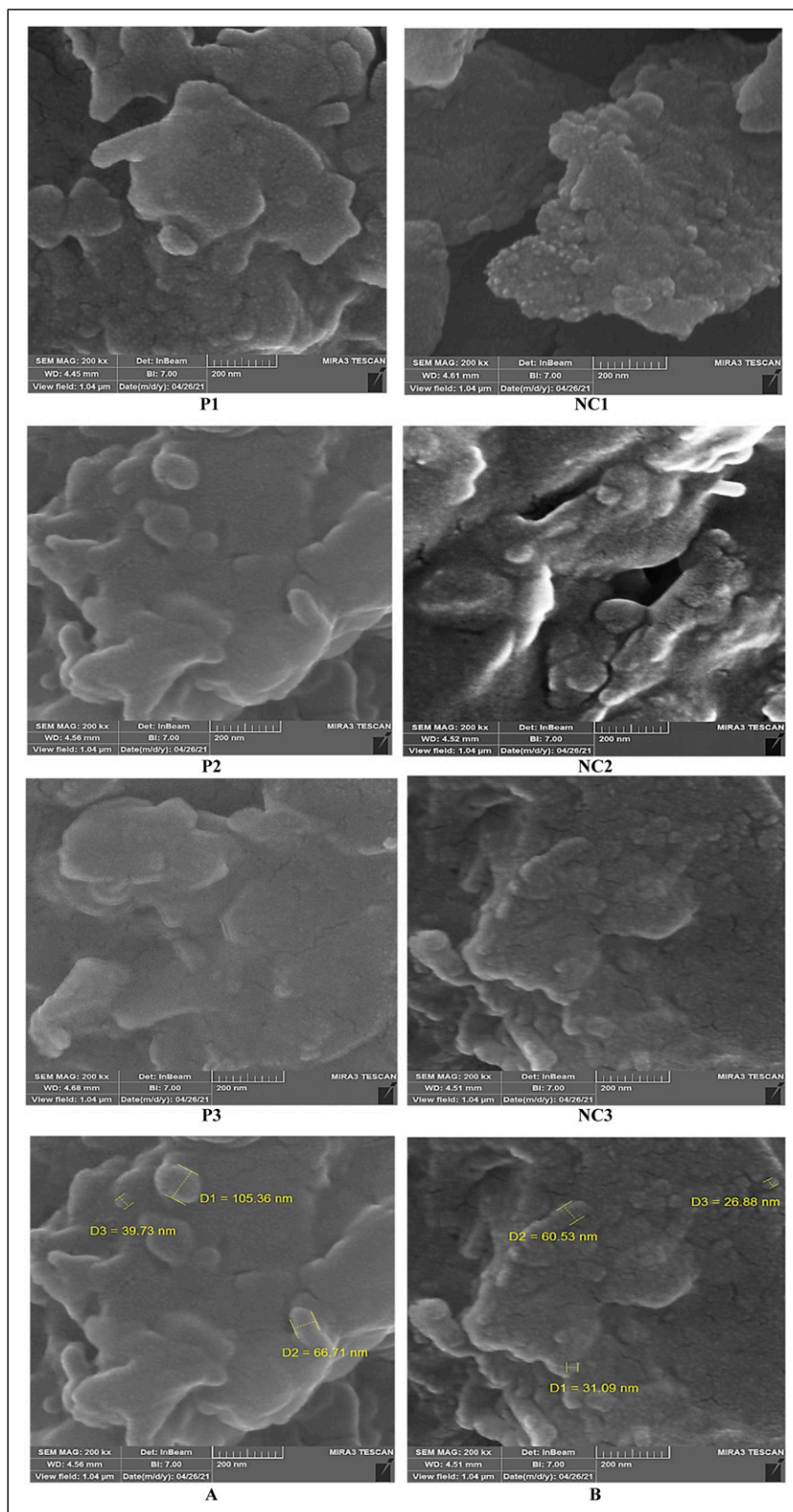
Figure 9. FESEM image of the sample surface, and (A and B) showed the nanosize of measurements in nanocomposites.

with matter which are the photoelectric effect, Compton scattering, and pair production.[45,46] Where the cross-sections for the photoelectric interactions are sufficiently high and photons are prone to be absorbed mainly by the photoelectric effect. Therefore, the loading of GO nanosheets in the polymer matrix that has a strong photon absorption capability of up to 2.3% for each graphene layer over a broad wavelength range, which makes it suitable for specific applications.[47] Materials with large mass amounts, high atomic numbers, and density were required for attenuation of the radiation rays for shielding application, therefore the addition of the GO nanosheets increased the mass per area in the radiation rays path that expects to exhibit better shielded due to it is the probability for absorption passed radiation-ray through the nanocomposites leads to an exponential decrease of intensity of pass radiation.[5] In comparison with the polymer-based results, the nanostructured GO nanosheets are
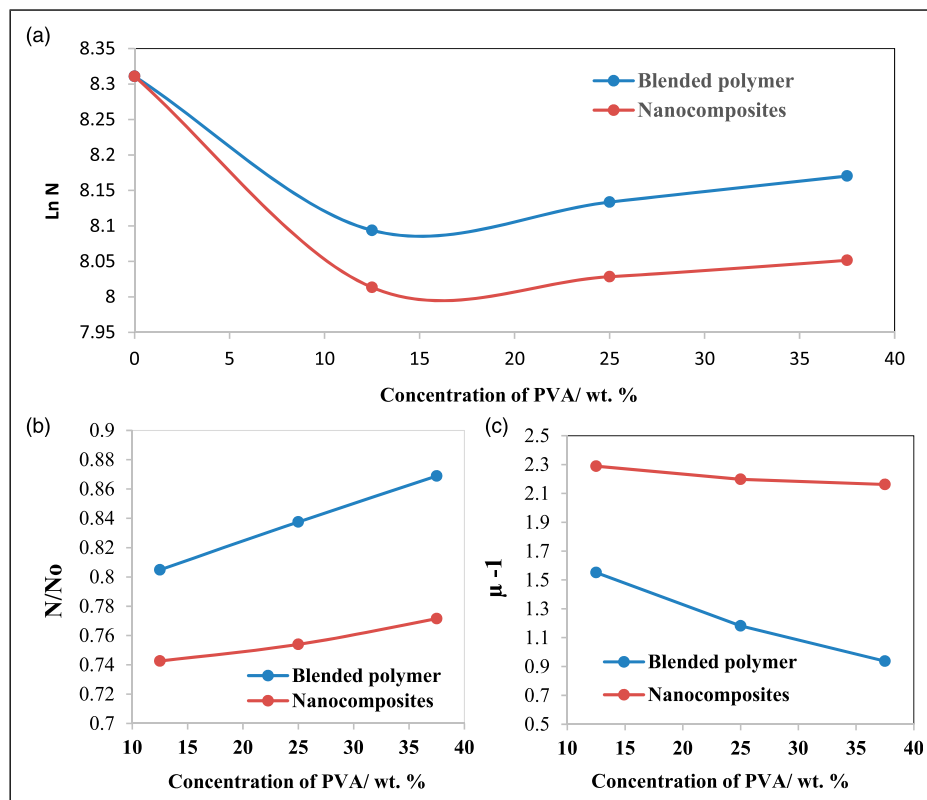
Figure 10. (a) The Ln of radiation attenuation (N), (b) the proportion between the radiation attenuation (N) with the radiation particles number (N_o) as (N/N_o), and (c) the attenuation of source radiation coefficient (μ) with increasing the PVA ratio of PEO-PVA blended polymer and nanocomposites.

an effective and efficient high-value-added alternative for use in radiation shielding materials in agreement with the other results that reported the use of the nanostructured materials that reduced the attenuation the gamma rays. They reported that nanocomposites and gamma photons influence one another, where nanocomposites with a higher ratio of nanostructures such as SeO_2,[48] CdO,[46] PbO,[49] GO,[5] and nano-$BaSO_4$[50] have better radiation attenuation properties that have a higher content of the polymer.

Conclusions

The developed methods successfully produced new nanocomposites fabricated from UHMWPEO with PVA and loaded with GO nanosheets. The nanocomposites reveal a good interfacial interaction between polymers and GO, as revealed by FTIR. The XRD spectra revealed a shifting in the polymer crystalline peaks after the change to a higher peaks position of PEO with increasing the loading ratio of PVA, whereas the contribution of GO nanosheets reduced the peaks position of the PEO in the polymer matrix. Additionally, GO contribution decreases the average crystal size of blended polymer PEO-PVA compared to the PEO. OM showed homogeneously blended polymers and fine dispersion of nanosheets in the polymer matrix, which was confirmed by the SEM images. The optical properties revealed a higher absorption of the samples containing a higher ratio of UHMWPEO. Where UHMWPEO presents an important absorption behavior that is significantly enhanced by increasing the concentration of UHMWPEO in both samples blended polymers and nanocomposites. GO exposed outstanding tunable of the energy gap where it turns the blended polymer from insulation to the semiconductor. Where energy gap values improved up to 160% of the nanocomposites. The results show improvement in optical properties, with the highest value of electromagnetic radiation absorption in the ultraviolet field (about 300 nm in wavelength). These results with notable absorption behviour and bandgap of the nanocomposites have the potential to contribute to solar cells, electronic devices, and a wide range of various applications. Furthermore, the contribution of both PVA and GO nanosheets has expressively improved the adsorption of the ray radiation compared with the blended polymers that make these materials promising for shielding applications.

Declaration of conflicting interests

The author(s) declared no potential conflicts of interest with respect to the research, authorship, and/or publication of this article.

Funding

ORCID iD

Ehssan Al-Bermany ⬤ https://orcid.org/0000-0002-7341-623X

Supplemental Material

Supplemental material for this article is available online.

References

1. Singh NB and Agarwal S. Nanocomposites: an overview. *Emerg Mater Res* 2016; 5(1): 5–43. Available from: https://www.icevirtuallibrary.com/doi/10.1680/jemmr.15.00025

2. Molaei P and Kazeminezhad I. One-step in situ synthesis of antimony sulfide/reduced graphene oxide composite as an absorber layer with enhanced photocurrent performances for solar cells. *J Nanoparticle Res* 2019; 21(3): 54. Available from: http://link.springer.com/10.1007/s11051-019-4490-9

3. Lee L, Zeng C, Cao X, et al. Polymer nanocomposite foams. *Compos Sci Technol* 2005; 65(15–16): 2344–2363. Available from: https://linkinghub.elsevier.com/retrieve/pii/S0266353805002253

4. Husain A, Ahmad S and Mohammad F. Polythiophene/graphene/zinc tungstate nanocomposite: Synthesis, characterization, DC electrical conductivity and cigarette smoke sensing application. *Polym Polym Compos* 2021; 29(6): 605–616. Available from: http://journals.sagepub.com/doi/10.1177/0967391120929079

5. Kadhim MA and Al-Bermany E. New fabricated PMMA-PVA/graphene oxide nanocomposites: Structure, optical properties and application. *J Compos Mater* 2021; 55(20): 2793–2806. Available from: http://journals.sagepub.com/doi/10.1177/0021998321995912

6. Cui F, Feng Q, Hong J, et al. Synthesis of large-size 1Tʹ ReS 2 x Se 2(1−x) alloy monolayer with tunable bandgap and carrier type. *Adv Mater* 2017; 29(46): 1705015. Available from: https://onlinelibrary.wiley.com/doi/10.1002/adma.201705015

7. Layek RK and Nandi AK. A review on synthesis and properties of polymer functionalized graphene. *Polymer (Guildf)* 2013; 54(19): 5087–5103. Available from: https://linkinghub.elsevier.com/retrieve/pii/S0032386113005636

8. Stankovich S, Dikin D a., Piner RD, et al. Synthesis of graphene-based nanosheets via chemical reduction of exfoliated graphite oxide. *Carbon N Y* 2007. [cited 2013 Oct 30];45(7):1558–65. Available from: https://linkinghub.elsevier.com/retrieve/pii/S0008622307000917

9. Stankovich S, Dikin DA, Dommett GHB, et al. Graphene-based composite materials. *Nature* 2006; 442(7100): 282–286. Available from: http://www.nature.com/articles/nature04969

10. Haghighi M, Khodadadi A, Golestanian H, et al. Effects of defects and functional groups on graphene and nanotube thermoset epoxy-based nanocomposites mechanical properties using molecular dynamics simulation. *Polym Polym Compos* 2021; 29(6): 629–639. Available from: http://journals.sagepub.com/doi/10.1177/0967391120929075

11. Wang H, Liu X, Yang Z, et al. Preparation and characterization of hexamethylenediamine-modified graphene oxide/Co-polyamide nanocomposites. *Polym Polym Compos* 2020; 28(6): 421–432. Available from: http://journals.sagepub.com/doi/10.1177/0967391119887298

12. Zheng YH, Han GC, Lu H, et al. Annealing temperature and thickness dependence of magnetic properties in epitaxial L1 0 -Mn 1.4 Ga films. *J Appl Phys* 2014; 115(4): 043902. Available from: http://aip.scitation.org/doi/10.1063/1.4862172

13. Tintu R, Saurav K, Sulakshna K, et al. Ge28Se60Sb12/PVA composite films for photonic applications. *J Non-oxide Glas* 2010; 2(4): 167–174.

14. Gomez-Barrena E, Puertolas J-A, Munuera L, et al. Update on UHMWPE research From the bench to the bedside. *Acta Orthop* 2008; 79(6): 832–840. Available from: http://www.tandfonline.com/doi/full/10.1080/17453670810016939

15. Drakopoulos SX, Psarras GC, Forte G, et al. Entanglement dynamics in ultra-high molecular weight polyethylene as revealed by dielectric spectroscopy. *Polymer* 2018; 150: 35–43. Available from: https://linkinghub.elsevier.com/retrieve/pii/S0032386118306165

16. Schmatloch S, van den Berg AMJ, Alexeev AS, et al. Soluble high-molecular-mass poly(ethylene oxide)s via self-organization. *Macromolecules* 2003; 36(26): 9943–9949. Available from: https://pubs.acs.org/doi/10.1021/ma0350359

17. Al-Abbas SS, Ghazi RA, Al-shammari AK, et al. Influence of the polymer molecular weights on the electrical properties of Poly(vinyl alcohol) – Poly(ethylene glycols)/Graphene oxide nanocomposites. *Mater Today Proc* 2021; 42(5): 2469–2474. Available from: https://linkinghub.elsevier.com/retrieve/pii/S2214785320402822

18. Saeedi F, Montazeri A, Bahari Y, et al. A study on the viscoelastic behavior of chitosan-polyvinyl alcohol-graphene oxide nano-composite films as a wound dressing. *Polym Polym Compos* 2021; 29(8): 1259–1272. Available from: http://journals.sagepub.com/doi/10.1177/0967391120962375

19. Hassan CM and Peppas NA. Structure and applications of poly(vinyl alcohol) hydrogels produced by conventional crosslinking or by freezing/thawing methods. In: *Biopolymers · PVA Hydrogels, Anionic Polymerisation Nanocomposites*. Berlin, Heidelberg: Springer Berlin Heidelberg, 2000, pp. 37–65. Available from: http://link.springer.com/10.1007/3-540-46414-X_2

20. Rajendran S, Sivakumar M and Subadevi R. Investigations on the effect of various plasticizers in PVA-PMMA solid polymer blend electrolytes. *Mater Lett* 2004; 58(5): 641–649. Available from: https://linkinghub.elsevier.com/retrieve/pii/S0167577X03005858

21. Kashyap S, Pratihar SK and Behera SK. Strong and ductile graphene oxide reinforced PVA nanocomposites. *J Alloys Compd* 2016; 684: 254–260. Available from: https://linkinghub.elsevier.com/retrieve/pii/S0925838816314955

22. Aziz SB, Abdullah OG, Hussein AM, et al. Optical properties of pure and doped PVA:PEO based solid polymer blend electrolytes: two methods for band gap study. *J Mater Sci Mater Electron* 2017; 28(10): 7473–7479. Available from: http://link.springer.com/10.1007/s10854-017-6437-1

23. Cao Y-C, Xu C, Wu X, et al. A poly (ethylene oxide)/graphene oxide electrolyte membrane for low temperature polymer fuel cells. *J Power Sourc* 2011: 196–282. Available from: https://linkinghub.elsevier.com/retrieve/pii/S0378775311013115

24. Hummers WS and Offeman RE. Preparation of graphitic oxide. *J Am Chem Soc* 1958; 80(6): 1339–1339. Available from: https://pubs.acs.org/doi/abs/10.1021/ja01539a017

25. Al-Bermany E and Chen B. Preparation and characterisation of poly(ethylene glycol)-adsorbed graphene oxide nanosheets. *Polym Int* 2021; 70(3): 341–351. Available from: https://onlinelibrary.wiley.com/doi/10.1002/pi.6140

26. Abdelamir AI, Al-Bermany E and Sh Hashim F. Enhance the optical properties of the synthesis PEG/graphene- based nanocomposite films using GO nanosheets. *J Phys Conf Ser* 2019; 1294(2): 022029. Available from: https://iopscience.iop.org/article/10.1088/1742-6596/1294/2/022029

27. Alias AN, Zabidi ZM, Ali AMM, et al. Optical characterization and properties of polymeric materials for optoelectronic and photonic applications. *Int J Appl Sci Technol* 2013; 3(5): 11. Available from: https://www.ijastnet.com/journals/Vol_3_No_5_May_2013/3.pdf

28. Pankove JI and Kiewit DA. Optical processes in semiconductors. *J Electrochem Soc* 1972; 119(5): 156C. Available from: https://iopscience.iop.org/article/10.1149/1.2404256

29. Suryawanshi VN, Varpe AS and Deshpande MD. Band gap engineering in PbO nanostructured thin films by Mn doping. *Thin Solid Films* 2018; 645: 87–92. Available from: https://linkinghub.elsevier.com/retrieve/pii/S0040609017307678

30. Qi G-Q, Liang C-L, Bao R-Y, et al. Polyethylene glycol based shape-stabilized phase change material for thermal energy storage with ultra-low content of graphene oxide. *Sol Energy Mater Sol Cells* 2014; 123: 171–177. Available from: https://linkinghub.elsevier.com/retrieve/pii/S0927024814000403

31. Jagtap SB, Kushwaha RK and Ratna D. Novel green method of preparation of a poly (ethylene oxide)/graphene nanocomposite using organic salt assisted dispersion. *RSC Adv* 2015; 5(39): 30555–30563. Available from: http://xlink.rsc.org/?DOI=C5RA01236H

32. Adhikari R and Michler GH. Polymer nanocomposites characterization by microscopy. *Polym Rev* 2009; 49(3): 141–180. Available from: http://www.tandfonline.com/doi/abs/10.1080/15583720903048094

33. Sun L and Fugetsu B. Mass production of graphene oxide from expanded graphite. *Mater Lett* 2013; 109(6): 207–210. Available from: http://arxiv.org/abs/1301.3253

34. Abdelamir AI, Al-Bermany E and Hashim FS. Important factors affecting the microstructure and mechanical properties of PEG/GO-based nanographene composites fabricated applying assembly-acoustic method. In: *AIP Conference Proceedings*, 2020, p. 020110. Available from: http://aip.scitation.org/doi/abs/10.1063/5.0000175

35. Al-shammari AK and Al-Bermany E. New fabricated (PAA-PVA/GO) and (PAAm-PVA/GO) nanocomposites: functional groups and graphene nanosheets effect on the morphology and mechanical properties. *J Phys Conf Ser* 2021; 1973(1): 012165. Available from: https://iopscience.iop.org/article/10.1088/1742-6596/1973/1/012165

36. Schadler L. Model interfaces. *Nat Mater* 2007; 6(4): 257–258. Available from: http://www.nature.com/articles/nmat1873

37. Maiti R, Midya A, Narayana C, et al. Tunable optical properties of graphene oxide by tailoring the oxygen functionalities using infrared irradiation. *Nanotechnology* 2014; 25(49): 495704. Available from: https://iopscience.iop.org/article/10.1088/0957-4484/25/49/495704

38. Li D, Müller MB, Gilje S, et al. Processable aqueous dispersions of graphene nanosheets. *Nat Nanotechnol* 2008; 3(2): 101–105. Available from: http://www.nature.com/articles/nnano.2007.451

39. Abutalib MM. Effect of additive concentration and X-ray irradiation on the thermal and color properties of Polyvinyl alcohol. *Life Sci J* 2014; 11(9): 512–517. Available from.chrome-extension://efaidnbmnnnibpcajpcglclefindmkaj/http://www.lifesciencesite.com/lsj/life1109/085_25952life110914_512_517.pdf

40. Desjardins SR, Penfield KW, Cohen SL, et al. Detailed absorption, reflectance, and UV photoelectron spectroscopic and theoretical studies of the charge-transfer transitions of tetrachlorocuprate(2-) ion: correlation of the square-planar and the tetrahedral limits. *J Am Chem Soc* 1983; 105(14): 4590–4603. Available from: https://pubs.acs.org/doi/abs/10.1021/ja00352a014

41. Hasan MT, Senger BJ, Ryan C, et al. Optical band gap alteration of graphene oxide via ozone treatment. *Sci Rep* 2017; 7(1): 6411. Available from: http://www.nature.com/articles/s41598-017-06107-0

42. Aldulaimi NR and Al-Bermany E. New fabricated UHMWPEO-PVA hybrid nanocomposites reinforced by GO nanosheets: structure and DC electrical behaviour. *J Phys Conf Ser* 2021; 1: 1973012164. Available from: https://iopscience.iop.org/article/10.1088/1742-6596/1973/1/012164

43. Chau JLH, Lin Y-M, Li A-K, et al. Transparent high refractive index nanocomposite thin films. *Mater Lett* 2007; 61(14–15): 2908–2910. Available from: https://linkinghub.elsevier.com/retrieve/pii/S0167577X07001140

44. Fortunati E, Luzi F, Puglia D, et al. Processing of PLA nanocomposites with cellulose nanocrystals extracted from Posidonia oceanica waste: Innovative reuse of coastal plant. *Ind Crops Prod* 2015; 67: 439–447. Available from: https://linkinghub.elsevier.com/retrieve/pii/S0926669015000771

45. Choppin G, Liljenzin J-O, Rydberg J, et al. Absorption of nuclear radiation. In: *Radiochemistry and Nuclear Chemistry*. Elsevier, 2013, pp. 163–208. Available from: https://linkinghub.elsevier.com/retrieve/pii/B9780124058972000070

46. El-Khatib AM, Abbas MI, Elzaher MA, et al. Gamma attenuation coefficients of nano cadmium oxide/high density polyethylene composites. *Sci Rep* 2019; 9(1): 16012. Available from: http://www.nature.com/articles/s41598-019-52220-7

47. Lewis CE. The training of new health manpower. *Acad Med* 1975; 50(12): 75–83. Available from: http://www.ncbi.nlm.nih.gov/pubmed/503

48. Cinan ZM, Erol B, Baskan T, et al. Radiation shielding tests of crosslinked polystyrene-b-polyethyleneglycol block copolymers blended with nanostructured selenium dioxide and boron nitride particles. *Nanomaterials* 2022; 12(3): 297. Available from: https://www.mdpi.com/2079-4991/12/3/297

49. Elsafi M, Sayyed MI, Almuqrin AH, et al. Analysis of particle size on mass dependent attenuation capability of bulk and nanoparticle PbO radiation shields. *Results Phys* 2021; 26: 104458. Available from: https://linkinghub.elsevier.com/retrieve/pii/S2211379721005738

50. Tekin HO, Singh VP, Kara Ü, et al. Investigation of nanoparticle effect on radiation shielding property using Monte Carlo method. *Celal Bayar Üniversitesi Fen Bilim Derg* 2016; 12(2): 195–199. Available from: http://dergipark.gov.tr/doi/10.18466/cbujos.15586